DEVELOPMENT OF A BAR-SHAPED ULTRASONIC MOTOR FOR MULTI-DEGREES OF FREEDOM MOTION

Kenjiro Takemura
KEIO University, Yokohama, Kanagawa, JAPAN, m982468@msr.st.keio.ac.jp
Nobuyuki Kojima
Canon Inc., Ohta-ku, Tokyo, JAPAN, kojima@ua.canon.co.jp
Takashi Maeno
KEIO University, Yokohama, Kanagawa, JAPAN, maeno@mech.keio.ac.jp

ABSTRACT
Small and precise actuators that enable multi-degrees of freedom (multi-DOF) are required in order to construct dexterous robot arms and manipulators. However, the total system of general electromagnetic motors used to generate multi-DOF motion is usually large and heavy. In contrast, ultrasonic motors are well-suited to multi-DOF actuation due to characteristics such as high output power per unit volume, high stationary limiting torque, high torque at low rotational speed, high controllability and simplicity of design. Several types of ultrasonic motors have been proposed that enable multi-DOF motion, most of which are not suitable for minimization because they use a large number of stators to generate multi-DOF motion.
In the present study, a three-DOF ultrasonic motor that uses a bar-shaped stator is developed. The three-DOF ultrasonic motor can be constructed when three natural frequencies of a bar-shaped stator are made to correspond. When two of these natural vibrations, two bending modes and a longitudinal mode, have a phase difference of 90 degrees, a spherical rotor in contact with the stator head rotates around three perpendicular axes. The structure of the ultrasonic motor is designed using finite element analysis. Measured natural frequencies and natural modes of vibration agree well with those calculated. In addition to the confirmation of three-DOF motion, the basic characteristics of the three-DOF ultrasonic motor, the rotational speed and load-velocity curve of the spherical rotor around three perpendicular axes were measured.

INTRODUCTION
Generating dexterous and precise actuation, such as that of human beings, is one of the targets of engineers working in the field of robotics. Needs for the actuators generating dexterous-precise motion are becoming increasingly necessary in the field of mechanical, electronical and medical engineering. Both the volume and weight of each actuator must be considered when designing a motion unit capable of generating multi-DOF motion. The total volume and weight of the general electromagnetic motor unit increase because gear trains used to reduce the rotational speed must be connected to the output axis. In addition, such motors require electric power even when the rotational speed is zero in order to generate a holding torque. Furthermore, the total number of motors required is equal to the number of DOF of motion. Thus, constructing a multi-DOF unit using general one-DOF actuators is difficult.
Various multi-DOF actuators that address these problems have been proposed. In particular, characteristics of ultrasonic motors such as high torque at low rotational speed that requires no gear trains to reduce the rotational speed and high stationary limiting torque that requires no electric power to maintain the position are well-suited to multi-DOF actuation. In addition, these motors offer the advantages of silence, simplicity of design, absence of electromagnetic waves, and high controllability. However, most ultrasonic motors proposed have only one-DOF, i.e., rotational or linear motion[1-3]. Toyama [4] developed a spherical ultrasonic motor in which three or four ring-shaped stators (vibrators) are arranged around a spherical rotor

in order to generate three- or two-DOF motion. However, the unused stators generate the excess load and heat when other stator in contact with the rotor is vibrating. Nakamura [5] proposed a bar-shaped ultrasonic motor capable of generating three-DOF motion. They generated three-DOF actuation using only one stator. However, the structure of the stator and the contact points of the stator/rotor are not optimized. Bansevicius[6] proposed a piezoelectric multi-DOF actuator. Six-DOF motion is generated using one stator. However, the construction of the stator is not simple enough for mass production. The present authors [7] propose a bar-shaped ultrasonic motor capable of three-DOF motion using one stator. Three natural vibrations of a bar-shaped stator are used. A spherical rotor in contact with the stator rotates around three perpendicular axes. The geometry of the bar-shaped stator is designed in detail using finite element analysis. In addition, the basic performance of the constructed bar-shaped ultrasonic motor is measured.

DESIGN

Geometry of the Stator

Former ultrasonic motors are frictionally driven motors in which two natural vibrations of the stator are excited at a phase difference of 90 degrees. These ultrasonic motors are of two types; the traveling wave type and the standing wave type. Two similar natural vibrations are used in the traveling wave type motor, and two different natural vibrations are used in the standing wave type motor. Points on the surface of the stators of former ultrasonic motors for one-DOF motion rotate in an oval locus when two natural frequencies of the stators correspond. The rotor in contact with the surface point of the stator is driven by frictional force. We introduce this driving principle to three-DOF motion. Namely, the stator design must meet the following requirements ;

1. The frequencies of three natural vibrations correspond.
2. Vibrating directions of a point on a stator for three natural vibrations are perpendicular each other, so that the moving plane of the three oval loci are perpendicular to each other.
3. The structure of the stator is simple and can be easily assembled and can be made small.
4. Three natural vibrations are simple, low order and have low frequencies, so that unnecessary vibration is not excited.

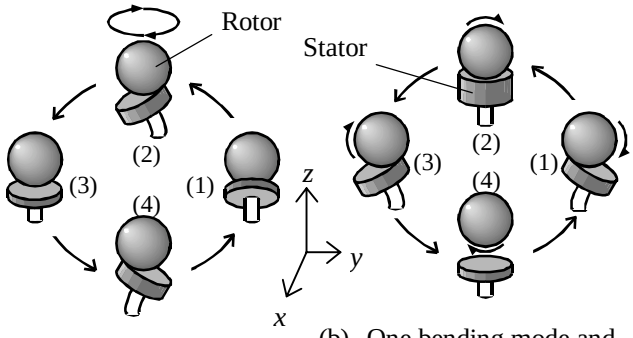

FIGURE 1: Principle of a multi-DOF ultrasonic motor

In the present study, a bar-shaped geometry of the stator was chosen because this geometry satisfies all of the above requirements. The natural vibration modes of the stator excited are two second bending modes and a first longitudinal mode. FIGURE 1 shows the driving principle of a bar-shaped ultrasonic motor. When two bending modes (1)(3) and (2)(4) are excited at a phase difference of 90 degrees, a spherical rotor rotates around the z-axis, as shown in FIGURE 1 (a). When a bending mode (1)(3) and a longitudinal mode (2)(4) are excited at a phase difference of 90 degrees, a spherical rotor rotates around the x-axis, as shown in FIGURE 1 (b). This bar-shaped ultrasonic motor is a hybrid motor, which acts as a traveling wave motor when two bending modes are used and as a standing wave motor when a bending mode and a longitudinal mode are used. The spherical rotor can be rotated around any axis by combining above three natural vibrations.

FIGURE 2 shows the structure of the bar-shaped multi-DOF ultrasonic motor designed using the finite element method. We used FE code MARC, and analyzed natural frequency and natural mode using the Lanczos method. The number of elements and nodes of the FE model are 5356 and 6729, respectively. The FE model and calculated natural modes of the stator are shown in FIGURE 3. The characteristics of the structure are as follows.

Location of Piezoelectric Ceramic

Three layers of piezoelectric ceramic (PZT) plates, two of which are for bending modes and one of which is for the longitudinal mode, are located between metal blocks. Each layer has three PZT plates, two of which excite the natural vibration and one of which detects the vibration.

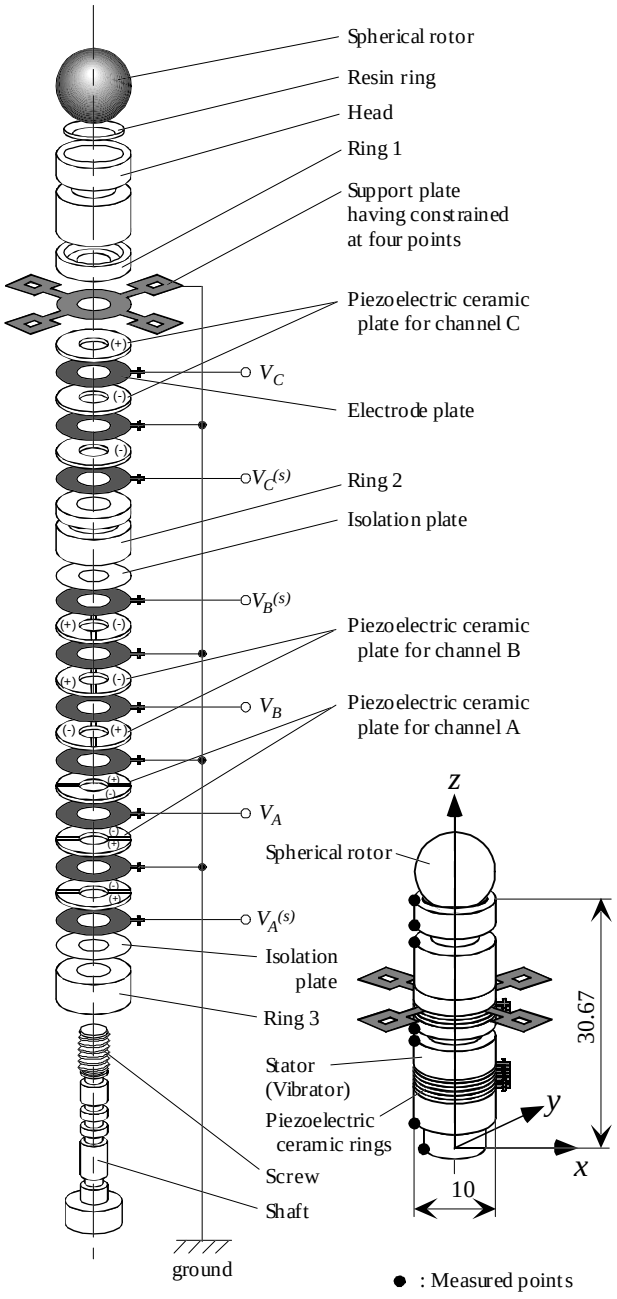

(a) Motor components (b) Entire view

FIGURE 2: Structure of a multi-DOF ultrasonic motor

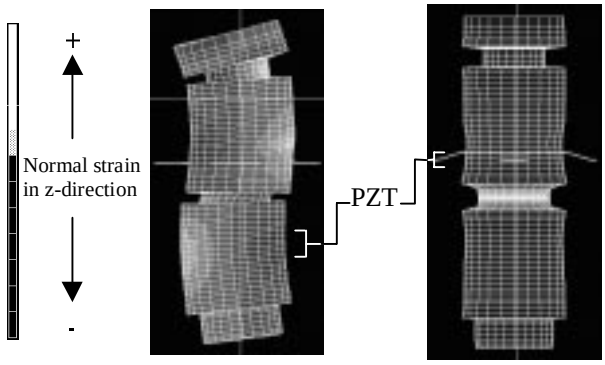

(a) 2nd bending mode (b) 1st longitudinal mode

FIGURE 3: Calculated natural modes of the stator on which the normal strain distribution is mapped

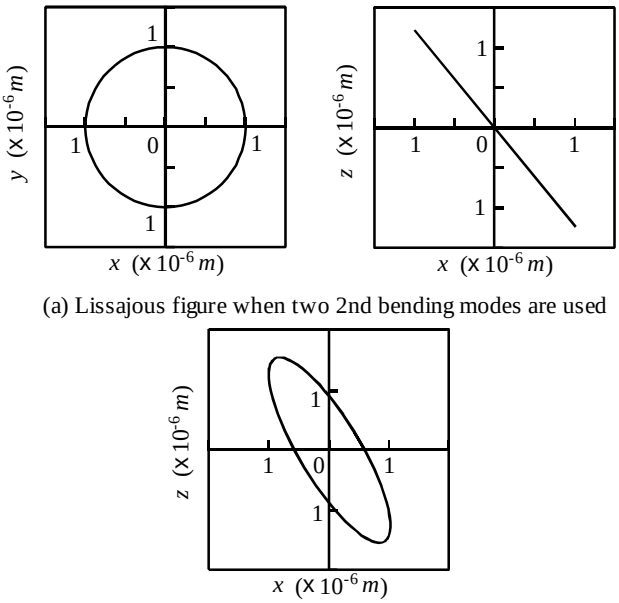

(a) Lissajous figure when two 2nd bending modes are used

(b) Lissajous figure when a 2nd bending mode and a 1st longitudinal mode are used

FIGURE 4: Lissajous figure at the contact point of the bar-shaped stator

Each natural vibration is excited when the input voltage is added on the electrode for which the frequency is nearly the same as the bending/longitudinal natural frequencies. FIGURE 3 shows the calculated natural modes of the stator on which the normal strain distribution is mapped. FIGURE 3 shows the position of the PZT that is used to excite each natural vibration. By placing a layer of PZT where the strain is high, the desired natural vibrations can be excited with high efficiency.

Geometry of Constrictions

Some ring-shaped parts of the stator have constrictions. These constrictions result in low stiffness; therefore, the amplitude of the natural vibrations is extended and the natural frequencies are low.

Normally, the constriction located where the strain is large lowers the natural frequency because the stiffness for the mode becomes low. FIGURE 3 shows the normal strain distribution in z-axial direction along with the natural modes. The strain is found to be large at the

constriction located near the tip of the stator in FIGURE 3 (a), which means that the constriction is effective for the second bending mode of the stator. However, the strain is large at the constriction located near the middle of the stator in FIGURE 3 (b), which means that this constriction is effective for the first longitudinal mode of the stator. The constriction located in head causes the natural frequency of the second bending mode of the stator to be low, and the constrictions in ring1/ring2 cause the natural frequency of the first longitudinal mode of the stator to be low. The natural frequencies of bending/longitudinal modes are made to correspond by changing the geometry of above mentioned constrictions.

Geometry of Contact Interface

The Lissajous figures, the locus of the contact point (x=4, y=0, z=30.17) when amplitudes of the contact points are $1x10^{-6}$ m as calculated using the results of finite element analysis are shown in FIGURE 4. FIGURE 4 (a) shows the Lissajous figure when two second bending modes, in the y-z plane and the z-x plane, are exited at a phase difference of 90 degrees. FIGURE 4 (b) shows the Lissajous figure when the second bending mode in the z-x plane and the first longitudinal mode are exited at a phase difference of 90 degrees. We can see that the latter Lissajous figure leans to the horizontal axis. Therefore, the tangent line of a spherical rotor at the contact point should be made parallel to the axis of the Lissajous figure. Thus the surface geometry of the resin ring is decided as a truncated corn.

Other Structural Characteristics

An axial load must be added between the stator and the rotor when the ultrasonic motors are driven. A magnet that has a diameter of 3 mm and a thickness of 1 mm is located at the head of the stator to add the normal load between the stator and the spherical rotor. The load is about 0.7 N when the clearance between the magnet and the spherical rotor is approximately 0.1mm. The magnitude of the load depends on the clearance.

A cross-shaped plate is located in the middle section of the stator in order to hold the stator with its four ends constrained. The position of the plate is determined using finite element analysis so that the influence of the constraint on the natural vibrations is small.

FIGURE 5: Picture of the stator

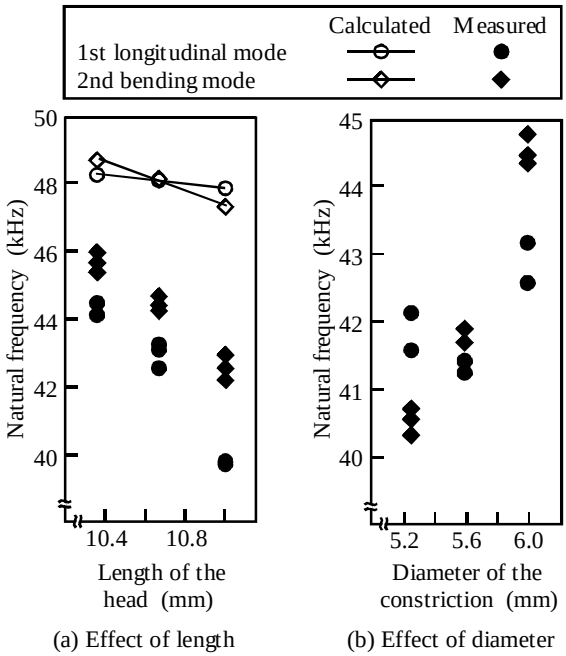

FIGURE 6: Calculated and measured natural frequencies of the stator

MEASUREMENT OF CHARACTERISTICS

Natural Vibrations of the Stator

A picture of the stator is shown in FIGURE 5. Several stators are produced by changing the diameter of the constriction located at the head and the length of the head, because there are the difference between the actual natural frequencies of the stator and those found using the FE result.

First, the natural frequencies of the stators are measured using an impedance gain phase analyzer. The measured natural frequencies are shown in FIGURE 6. FIGURE 6 (a) shows the natural frequencies when the length of head is changed and the diameter of constriction is 6 mm. FIGURE 6 (b) shows the natural frequencies when the diameter of constriction is changed and the length of the head is 10.665 mm (Unchanged parameters are

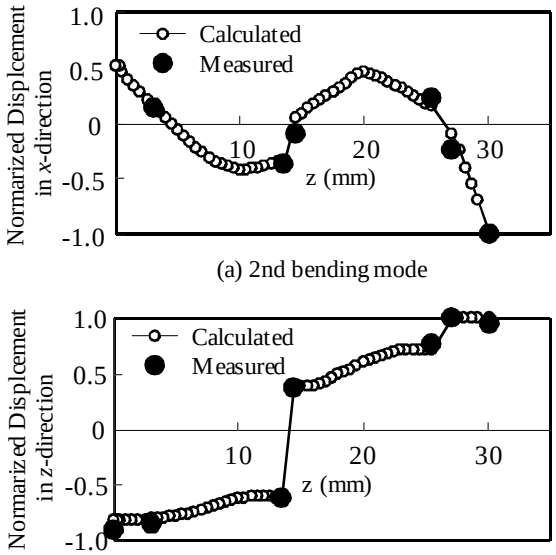

(a) 2nd bending mode

(b) 1st longitudinal mode

FIGURE 7: Calculated and measured natural modes of the stator

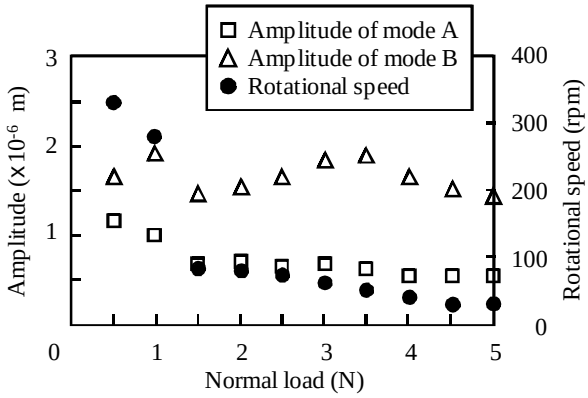

(a) When two 2nd bending modes are used

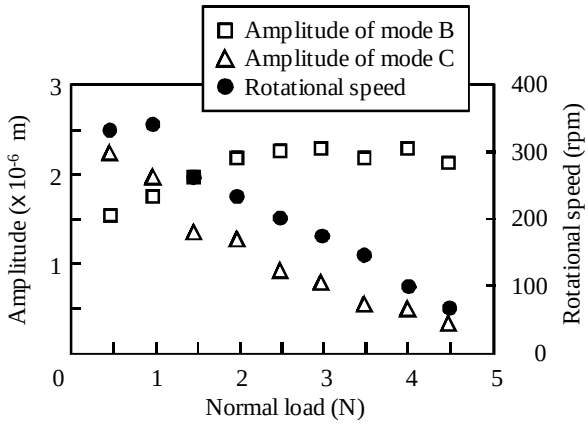

(b) When one 2nd bending mode and one 1st longitudinal mode are used

FIGURE 8: Measured rotational speed and amplitude of the motor when the normal load is changed

equal to those used in the finite element model). The measured values are about 10% lower than those calculated. The reason for this is that the boundaries between parts are not modeled. For the stator that has a head length of 10.665mm and a constriction diameter of 5.6mm, the difference in natural frequencies between the second bending mode and the first longitudinal mode is less than 500 Hz.

Next, the natural modes of the stator are measured (parameters are the same as those used in the finite element model) using an optical displacement measuring system. FIGURE 7 shows the displacements of the measured points (shown in FIGURE 2) when the second bending mode and the first longitudinal mode are excited. The displacements are normalized by dividing them by the maximum values in FIGURE 7. The measured displacements of the points agree well with the calculated displacements.

Driving Characteristics

We confirm that a spherical rotor can be rotated around three perpendicular axes with expected performance using a stator having natural frequencies within 500 Hz.

A measurement system was developed in order to measure the basic driving characteristics of the spherical rotor. The torque and rotational speed of the spherical rotor can be measured around three perpendicular axes using this device. The load between the stator and the rotor can also be changed. The magnet was removed from the motor during this measurement. The rotational speed was measured when the input electronic power was 40 V. FIGURE 8 shows the maximum rotational speed of the spherical rotor around perpendicular axes and the amplitude of the stator head when the frequencies of input power are swept from 45 kHz to 41 kHz. The rotational speed decreases as the load increases. The amplitudes is also thought to decrease as the load increases. However, the amplitude of mode B does not show this tendency. The reason for this is that the load during the measurement was not equal around the contact area due to error in the processing method or the measuring device.

FIGURE 9 shows the torque-rotational speed curve obtained when the spherical rotor was driven around the perpendicular axes. The input voltage was 40 V. The load between the stator and the rotor was 3 N. The

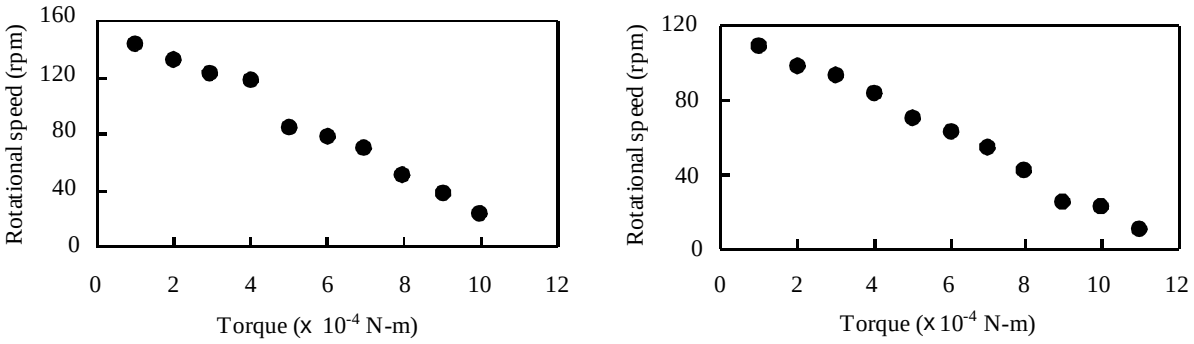

(a) When two 2nd bending modes are used

(b) When one 2nd bending mode and one 1st longitudinal mode are used

FIGURE 9: Measured T-N curve of the motor

frequency of input electronic power is 42.47 kHz when the two second bending modes are used, and 42.38 kHz when the second bending mode and the first longitudinal mode are used. As shown in FIGURE 9, the rotational speed decreases as the output torque decreases. This tendency is the same as that of former ultrasonic motors, but output torque is smaller for the proposed motor. A bar-shaped ultrasonic motor can generate an output torque of about 0.01 N-m when the load between stator and rotor is 4 N. In order to obtain lager output power, the structure of the stator/rotor contact point and the material of the resin ring should be improved.

CONCLUSIONS

In the present study, we proposed a multi-DOF ultrasonic motor and the structure of the stator for the ultrasonic motor. In addition, we measured the basic driving characteristics of the spherical rotor around the perpendicular axes. The spherical rotor can be rotated around three perpendicular axes using a bar-shaped stator for which the natural frequencies of the second bending mode and the first longitudinal mode correspond approximately. Since, the output power is smaller than that of the former bar-shaped ultrasonic motor, stator/rotor contact conditions should be optimized in future studies.

REFERENCES

1. I. Okumura, A Design Method of a Bar-Type Ultrasonic Motor for Autofocus Lenses, Proc. IFToMM-jc Intl. Symp. on Theory of Machines and Mechanisms, pp. 75-80, 1992
2. K. Nakamura *et al.*, Ultrasonic Motor Using Free Bending Vibration of a Short Cylinder, Journal of the Acoustical Society of Japan, pp. 795-796, 1988 (in Japanese)
3. Y. Tomikawa *et al.*, Same Phase Drive Type Ultrasonic motor, Proc. 7th Meeting on Ferroelectric Materials and Their Applications, Kyoto 1989, Japanese Journal of Applied Physics, Vol. 28 Supplement 28-2, pp. 198-201, 1989
4. S. Toyama *et al.*, Development of an Actuator for a Robotic Manipulator with Ultrasonic Motor –2nd Development of Prototypal Spherical Ultrasonic Motor-, Journal of the Robotics Society of Japan, Vol. 13, No. 2, pp. 235-241, 1995 (in Japanese)
5. K. Nakamura *et al.*, Designs of an Ultrasonic Actuator with Multi-degree of freedom using Bending and Longitudinal Vibrations (II), Journal of the Acoustical Society of Japan, pp. 376-377, 1998 (in Japanese)
6. R. Bansevicius, Piezoelectric Multi-degree of Freedom Actuators/Sensors, Proc. 3rd International Conference on Motion and Vibration Control, pp. K9-K15, 1996
7. T. Maeno and K. Takemura, Ultrasonic Motors with Multi-Degrees of Freedom using Longitudinal and Lateral Vibration, The 75th JSME Spring Annual Meeting (IV), pp. 637-638, 1998 (in Japanese)